Author/s:
Kragten, NAM;Behr, FM;Vieira Braga, FA;Remmerswaal, EBM;Wesselink, TH;Oja, AE;Hombrink, P;Kallies, A;van Lier, RAW;Stark, R;van Gisbergen, KPJM

Title:
Blimp-1 induces and Hobit maintains the cytotoxic mediator granzyme B in CD8 T cells

Date:
2018-10-01

Citation:
Kragten, N. A. M., Behr, F. M., Vieira Braga, F. A., Remmerswaal, E. B. M., Wesselink, T. H., Oja, A. E., Hombrink, P., Kallies, A., van Lier, R. A. W., Stark, R. & van Gisbergen, K. P. J. M. (2018). Blimp-1 induces and Hobit maintains the cytotoxic mediator granzyme B in CD8 T cells. European Journal of Immunology, 48 (10), pp.1644-1662. https://doi.org/10.1002/eji.201847771.

Blimp-1 induces and Hobit maintains the cytotoxic mediator granzyme B in CD8 T cells

Natasja A.M. Kragten[1*], Felix M. Behr[1,2*], Felipe A. Vieira Braga[1], Ester B. M. Remmerswaal[2,3], Thomas H. Wesselink[1], Anna E. Oja[1], Pleun Hombrink[1], Axel Kallies[4,5], Rene A.W. van Lier[1], Regina Stark[1,2], and Klaas P.J.M. van Gisbergen[1,2,4,5]

[1]Dept of Hematopoiesis, Sanquin Research and Landsteiner Laboratory AMC/UvA, Amsterdam, Netherlands; [2]Dept of Experimental Immunology, Academic Medical Center, Amsterdam, Netherlands; [3]Renal Transplant Unit, Academic Medical Center, Amsterdam, Netherlands; [4]The Walter and Eliza Hall Institute of Medical Research, Melbourne, Australia; [5]Dept of Microbiology and Immunology, The University of Melbourne, The Peter Doherty Institute for Infection and Immunity, Melbourne, Australia.

[*] Shared first authorship

Corresponding Author:

Klaas P.J.M. van Gisbergen

Tel: 0031-205123976

Fax: 0031-205123474

E-mail: k.vangisbergen@sanquin.nl

Keywords: Blimp-1, Hobit, CD8$^+$ T cells, granzyme B, cytotoxicity

Abstract:

CD8 T cells acquire cytotoxic molecules including granzyme B during effector differentiation. Both tissue-resident memory CD8 T cells (Trm) and circulating CD45RA+ effector-type T cells (Temra) cells have the ability to retain granzyme B protein expression into the memory phase, but it is unclear how this persistence of cytolytic activity is regulated during steady state. Previously, we have described that the transcriptional regulators Hobit and Blimp-1 have overlapping target genes that include granzyme B, but their impact on the regulation of cytotoxicity in Trm and Temra cells during homeostasis has remained unclear. We examined the expression regulation of Hobit and Blimp-1 in murine and human CD8 T-cells to determine their timeframe of activity. While Blimp-1 mRNA was expressed throughout effector and memory T cells, Blimp-1 protein, was only transiently expressed during the effector stage. In contrast, Hobit mRNA and protein expression was stably maintained during quiescence, but downregulated after activation. Notably, Blimp-1 was required for expression of granzyme B in murine effector T cells and Trm, while Hobit specifically regulated granzyme B in murine Trm during the memory phase. These findings suggest that Blimp-1 initiates cytotoxic effector function and that Hobit maintains cytotoxicity in a deployment-ready modus in Trm.

Introduction:

CD8 T cells provide an important line of immune defense in viral infection through their ability to eliminate infected cells in an antigen-specific manner. Naive CD8 T cells that recognize viral antigens are triggered to proliferate and differentiate into effector cells

within the lymph nodes. The effector cells migrate to the site of infection, where they produce pro-inflammatory cytokines, including IFN-γ and TNF-α, and cytotoxic molecules that assist in clearance of infected cells. Effector CD8 T cells engage two major pathways to induce killing of target cells that are mediated through surface-expressed death receptors such as the FasL/Fas and Trail/Trail-R ligand/receptor pairs and through secretory granules containing perforin and granzymes (1,2). Recognition of antigen in the context of MHC class I molecules triggers CD8 T cells to establish an immunological synapse with target cells that enables the directional release of cytotoxic granules and results in killing of infected cells, but not of uninfected cells. Granule-dependent cytotoxicity is driven by the pore-forming protein, perforin, which enables the release of proteolytic granzymes into the cytoplasm of target cells. Granzymes consist of a family of serine proteases, of which granzyme A and B have most clearly been associated with the induction of cytotoxicity (3). In mice, the importance of granule-mediated cytotoxicity has been shown by targeted disruption of perforin, which impairs viral clearance after infection with lymphocytic choriomeningitis virus (LCMV) and increases the incidence of carcinogen-induced and spontaneous cancers (4,5). The effects of deficiency in granzyme A or B are similar, but less dramatic than those of perforin ablation, suggesting substantial redundancy between members of the granzyme family (6).

After clearance of the infection, the effector population contracts into long-lived memory populations that enable more powerful responses upon secondary challenge. Central memory (Tcm), effector memory (Tem) and CD45RA+ effector-type cells (Temra) have been identified as separate long-lived CD8 T cell subsets that are maintained during quiescence in human peripheral blood (7,8). The peripheral tissues including the epithelial layers of skin,

lungs and intestine, but also internal organs such as brain, liver and kidney harbor tissue-resident memory CD8 T cells (Trm) that form separate populations distinct from the circulating Tcm, Tem and Temra populations (9). Tcm and Tem are important for immune surveillance of the lymphoid and peripheral tissues, respectively. These memory populations effectively mount secondary effector responses upon pathogen re-encounter (8). In contrast, Trm and Temra have limited proliferative capacity and provide protection against re-infection through their superior potential to rapidly up-regulate effector functions including the production of pro-inflammatory cytokines (7,10-12).

In contrast to effector cells, memory cells are maintained long-term in the absence of antigenic and inflammatory stimuli, which places constraints on the continuous production of effector molecules. Therefore, granzyme B-driven cytotoxicity is strongly down-regulated in in some populations of memory cells compared to effector cells (13). Tcm and the majority of Tem do not express granzyme B and perforin at the protein level, although epigenetic remodeling of the granzyme B locus suggests that it is more easily accessible in these circulating memory cells compared to naive cells (14,15). Indeed, Tcm and Tem maintain elevated expression of granzyme B mRNA compared to naive cells, but require additional signals to up-regulate granzyme B protein and establish cytotoxicity (13). Temra and Trm mediate border patrol of the endothelial and epithelial tissues, respectively, and therefore, require the persistence of direct effector functions to eliminate infected cells. In contrast to Tcm and Tem, Temra have been shown to express granzyme B and perforin at the protein level and are able to kill specific target cells without prior activation (7), suggesting that these cells display immediate cytotoxic potential after encounter of infected cells. Similarly, Trm that develop in the small intestine and brain after acute infection with

LCMV have been reported to express granzyme B during quiescence (16,17). Thus, a substantial fraction of the long-lived CD8 T cell populations has the potential to immediately engage granzyme B-driven cytotoxicity.

For the improvement of CD8 T cell therapies, it is highly relevant to understand how the immediate cytotoxic potential is maintained in the memory phase. However, at present, the regulation of granzyme B-driven cytotoxicity in Temra and Trm populations is unclear. Previously, we have demonstrated that Hobit is a transcriptional regulator that drives the expression of granzyme B in NKT cells (18). Interestingly, the expression of Hobit perfectly aligns with long-lived cytotoxic populations, as Hobit is specifically upregulated in Trm and human Temra cells within the CD8 T cell lineage (19,20). Hobit is highly homologous to the transcription factor Blimp-1, which has previously been shown to induce terminal differentiation in the B and T cell lineages (21). Furthermore, Blimp-1 is also involved in the acquisition of the full repertoire of effector functions, as it induces the production of granzyme B in CD8 T cells during the peak of the primary response (22-24). Effector CD8 T cell differentiation is under the control of a set of transcription factors that collaboratively regulate the separation of the short-lived effector (SLEC) and memory precursor (MPEC) lineages. Blimp-1 essentially contributes together with T-bet, Id2 and Notch to the development of SLECs (22-26). We therefore examined the roles of Hobit and Blimp-1 in the instruction of cytotoxicity in CD8 T cells. Strikingly, we found that the Hobit and Blimp-1 driven regulation of granzyme B expression is initiated at different stages of CD8 T cell differentiation.

Results:

Resident memory CD8 T cells maintain expression of cytotoxic molecules and cytotoxicity

Circulating populations of memory CD8 T cells in mice do not maintain the capacity to immediately lyse target cells (13). To determine the cytotoxic potential of Trm, we analyzed the ability of LCMV-specific CD8 T cells to mediate lysis of EL4 target cells loaded with cognate peptide. Given that sizeable populations of both Tem and Trm are present in the liver after LCMV infection, we analyzed the cytotoxic potential of these subsets. Virus-specific Trm displayed cytotoxic activity within 4 hours after stimulation in contrast to virus-specific Tem, which did not (Fig. 1A). Both Tem and Trm killed target cells after 24 hours (Fig. 1B), suggesting that Tem, despite the lack of immediate killing capacity can acquire cytotoxic effector function at later time-points. To study how Trm maintain the capacity to directly employ cytotoxicity, the expression of cytotoxic effector molecules in memory CD8 T cells was analyzed at late time-points after LCMV infection. Comparison of memory populations after LCMV infection using RNA sequencing showed that *Ifng* and cytotoxicity-associated molecules including *Gzmb* (granzyme B), *Gzmk* (granzyme K), *Fasl* (Fas ligand) and *Tnfsf10* (Trail) were strongly upregulated in gut and liver Trm compared to circulating memory populations (Fig. 1C). To further study the expression of cytotoxicity-associated molecules during primary CD8 T cell responses, virus-specific CD8 T cells were followed over time after acute infection with LCMV WE and LCMV Armstrong. The expression of granzyme B protein was detectable in effector CD8 T cells at day 8 post infection (p.i.) in spleen, liver and gut (Fig. 1, D and E; Suppl. Fig. 1A). Expression of granzyme B protein was partially maintained within LCMV-specific Trm from liver and gut, but not within LCMV-specific Tem from spleen and liver (Fig. 1, D-F; Suppl. Fig 1B). Similar to granzyme B, Fas ligand protein

was enriched on liver Trm compared to Tem (Fig. 1G). In contrast, protein expression of Trail was not detectable on these memory populations in contrast to resident NK cells (Fig. 1H; Suppl. Fig. 2). Granzyme B and Fasl mediate important pathways that enable cytotoxic T cells to eliminate target cells (1,2), suggesting that Trm in contrast to circulating memory cells maintain expression of these cytotoxic molecules at the protein level thereby enabling the direct elimination of infected cells after secondary infection.

Blimp-1 protein is transiently expressed in effector CD8 T cells to induce granzyme B expression

Blimp-1 is an important transcriptional regulator of cytotoxicity in effector CD8 T cells through its essential role in the induction of granzyme B expression (22-24,27). Blimp-1 is induced in CD8 T cells during effector differentiation (22,23). Transcriptional expression of Blimp-1 is maintained in memory CD8 T cells (22,23) including Trm (19), suggesting that Blimp-1 may also mediate transcriptional regulation of granzyme B in Trm. We assessed the contribution of Blimp-1 to the regulation of granzyme B expression in the memory phase using LCMV Armstrong rather than LCMV WE, as Blimp-1 deficient mice were only able to clear infection with this LCMV strain (unpublished observations). In line with previous findings (23,28), Blimp-1 was required for granzyme B expression in effector CD8 T cells at day 8 after LCMV infection (Fig. 2, A and B). Strikingly, the expression of granzyme B in Trm of liver and gut at day 36 p.i. was also largely dependent on Blimp-1 (Fig. 2, C and D). Blimp-1 deficiency did not compromise Trm formation, suggesting that Blimp-1 was essential for granzyme B expression rather than for the formation of granzyme B+ Trm (Suppl. Fig. 3, A-D). The timing of the requirement for Blimp-1 in the regulation of granzyme B expression in Trm was unclear. Given that Blimp-1 is already required for granzyme B expression during

the effector stage, it was possible that the early defect in Blimp-1 deficient effector CD8 T cells is retained in Trm. To address at which time-point Blimp-1 is most relevant, we analyzed the kinetics of Blimp-1 expression during CD8 T cell differentiation. Blimp-1 GFP and YFP reporter mice have been used to identify the expression profile of Blimp-1 in CD8 T cells (23,28). In line with reported data using Blimp-1 reporter mice, we found that Blimp-1 mRNA is up-regulated in effector CD8 T cells and maintained in effector memory and resident memory CD8 T cell populations (Fig. 3A). Blimp-1 expression also persists in central memory CD8 T cells, but at lower levels compared to effector CD8 T cells (Fig. 3A). Given that expression of Blimp-1 protein rather than mRNA is critical for Blimp-1 activity, we analyzed Blimp-1 at the protein level using flow cytometry. As expected, we observed Blimp-1 protein expression in plasma cells within the bone marrow (Fig. 3, B and C; Suppl. Fig. 4A and 5), in SLECs and MPECs of spleen (Fig. 3, D and E; Suppl. Fig. 4B and 6) and in effector CD8 T cells of the liver and small intestine (Fig. 3, F and G; Suppl. Fig. 4C), but not in naive CD8 T cells within the same tissues. However, memory CD8 T cells including Tcm and Tem populations in spleen (Fig. 3, H and I; Suppl. Fig. 4D), and Tem and Trm populations in the liver and small intestine (Fig. 3, J and K; Suppl. Fig. 4E) displayed undetectable or low expression of Blimp-1 protein. Thus, Blimp-1 protein in contrast to Blimp-1 mRNA is transiently induced in CD8 T cells during effector differentiation, suggesting that Blimp-1 acts early in the regulation of cytotoxicity. Therefore, the compromised granzyme B production in Blimp-1 deficient Trm appears to result from the early defect in the effector stage.

Hobit drives granzyme B expression during the memory phase in Trm

In mice, expression of Hobit, similar to that of granzyme B is confined to Trm within the CD8 T cell lineage (19), indicating that the close association between these molecules is conserved between mice and humans. As previously published (19), Hobit does not impact on Trm formation on its own (Suppl. Fig. 7, A-D), which provides opportunity to study the role of this transcription factor in the regulation of granzyme B in Trm. Hobit, in contrast to Blimp-1, was not required for granzyme B expression in effector CD8 T cells at day 8 after LCMV-WE infection (Fig. 4, A and B). However, the expression of granzyme B in Trm of liver and gut at day 61 p.i. was largely dependent on Hobit (Fig. 4, C and D). We observed that expression of granzyme B was compromised at the RNA level in Trm of Hobit KO mice, suggesting that Hobit was essential for the transcriptional regulation of granzyme B (Fig. 4E). Granzyme B is stored together with the pore-forming molecule perforin in secretory vesicles that contain the lysosomal protein LAMP-1/CD107a (13). In contrast to granzyme B, the expression of perforin was not dependent on Hobit (Fig. 4F). Peptide re-stimulation of virus-specific cells at day 61 after LCMV infection induced normal degranulation of CD107a+ vesicles in liver-derived Trm in the absence of Hobit (Fig. 4, G and H), indicating that Hobit controls cytotoxicity specifically through the transcriptional regulation of granzyme B expression. Hobit was also not involved in the regulation of other cytotoxic molecules including FasL (Suppl. Fig. 8, A and B). These findings show that Hobit specifically regulates granzyme B expression in CD8 T cells at late time-points after infection. Thus, whereas Blimp-1 is mandatory for the induction of granzyme B expression, Hobit rather than Blimp-1 appears important for the long-term maintenance of granzyme B expression in memory CD8 T cells.

Blimp-1 induces and Hobit maintains granzyme B expression in NKT cells

To examine whether the Hobit and Blimp-1 driven regulation of granzyme B expression was conserved between lymphocyte subsets, we analyzed the role of these transcription factors in NKT cells. NKT cells were taken for comparison, as we have shown previously that these cells share a Hobit and Blimp-1-driven transcriptional program of tissue residency with Trm (19). We first addressed the expression regulation of Blimp-1 in NKT cells. Blimp-1 mRNA expression, as reported using Blimp-1 GFP mice, was found in NKT cells under steady state and persisted at reduced levels in NKT cells after antigenic stimulation with α-galactoceramide (α-GalCer; Fig. 5A; Suppl. Fig. 9). In contrast to Blimp-1 mRNA, Blimp-1 protein was not abundant in NKT cells under steady state conditions, but was strongly induced after *in vivo* activation with α-GalCer (Fig. 5B). To study the maintenance of Blimp-1 expression, NKT cells were stimulated *in vitro* with anti-CD3/28 and IL-2 and subsequently rested in IL-15. Blimp-1 mRNA expression was maintained during culture as evidenced using GFP expression in Blimp-1 reporter mice (Fig. 5C). At the protein level, Blimp-1 was present 2 days, but not 6 days, after removal of antigen (Fig. 5D). These findings suggest that Blimp-1 protein is transiently induced in NKT cells after antigenic activation. Thus, the regulation of Blimp-1 expression appears to be conserved between CD8 T cell and NKT cell lineages. A subset of WT NKT cells up-regulated granzyme B expression after *in vivo* antigenic activation with α-GalCer for 3 days (Fig. 6, A and B). The expression of granzyme B in NKT cells under these conditions was largely dependent on Blimp-1, as shown by the strongly impaired granzyme B response in Blimp-1 deficient compared to WT NKT cells (Fig. 6, A and B). We have previously shown that thymic NKT cells express granzyme B during steady state in a Hobit dependent manner (18). These findings suggest that Hobit regulates granzyme B in NKT cells under resting conditions and Blimp-1 after antigenic stimulation. After *in vitro*

stimulation with anti-CD3/28 and IL-2 NKT cells also up-regulated granzyme B and expression was dependent on Hobit and Blimp-1, but only partially (Fig. 6, C and D). We made use of cultured NKT cells to determine the maintenance requirements of granzyme B expression. Congenically marked NKT cells were analyzed more than 2 weeks after adoptive transfer into recipient mice. Hobit or Blimp-1 deficient NKT cells were normally maintained compared to WT NKT cells, as published previously (19). Expression of granzyme B was persistent in WT and Blimp-1 deficient NKT cells. In contrast, Hobit deficient NKT cells largely lost expression of granzyme B (Fig. 6, E and F). Thus, Hobit rather than Blimp-1 mediates persistence of granzyme B expression in NKT cells.

Regulation of Blimp-1 expression in human CD8 T cells

In contrast to circulating memory CD8 T cells in mice, a large fraction of memory and effector-type CD8 T cells (Temra) from human peripheral blood express high levels of granzyme B and perforin protein under steady state conditions (29). The transcription factors involved in the regulation of granzyme B and perforin expression in quiescent memory and effector-type CD8 T cells remain unclear. To determine the potential role of Blimp-1 in this process, we examined the expression of Blimp-1 in cytotoxic CD8 T cell populations in humans. For this purpose, we set up an *in vitro* culture protocol of human CD8 T cells (Fig. 7A). We found that Blimp-1 mRNA was expressed in memory and quiescent effector-type CD8 T cells in contrast to naive CD8 T cells (Fig. 7B), as previously reported (30). Despite the abundant presence of Blimp-1 mRNA, we observed that Blimp-1 protein expression was nearly absent in memory CD8 T cells (Fig. 7C). Although activation using anti-CD3/28 antibodies in combination with IL-2 did not further increase expression of Blimp-1 mRNA in memory CD8 T cells (Fig. 7B), Blimp-1 protein was strongly induced in these cells

(Fig. 7C). These findings suggest that Blimp-1 activity in memory cells is regulated at the protein level and requires antigenic stimulation. To study the maintenance of Blimp-1 expression after activation, we initially stimulated naive human CD8 T cells using anti-CD3/28 and IL-2, before resting them in the presence of the homeostatic cytokine IL-15 (Fig. 7A). Naive CD8 T cells upregulated Blimp-1 mRNA and protein after stimulation (Fig. 7, B and C). After resting of the cells, Blimp-1 mRNA expression was largely maintained (Fig. 7D), but Blimp-1 protein expression was rapidly lost (Fig. 7E). The longitudinal analysis indicated that Blimp-1 persists at the mRNA level, but not at the protein level after removal of antigenic stimuli, suggesting that Blimp-1 activity is confined to situations where TCR-stimulation occurs. Taken together, these findings suggest that alternative Blimp-1 independent pathways regulate granzyme B expression and cytotoxicity in CD8 T cells during quiescence in human and mouse CD8 T cells.

Hobit is expressed in granzyme B producing human CD8 T cells under resting conditions

Granzyme B clustered together with Hobit in microarray analysis of human memory and long-lived effector-type CD8 T cells, suggesting a role for this transcription factor in the regulation of cytotoxicity during quiescence (20,30). To address these findings at the protein level, we co-stained CD8 T cells from human peripheral blood for Hobit and granzyme B. Underlining the transcriptional profiling, a strong association between Hobit and granzyme B was found at the protein level. The majority of Hobit+ CD8 T cells co-expressed granzyme B and vice versa the majority of granzyme B+ CD8 T cells co-expressed Hobit (Fig. 8, A and B; Suppl. Fig. 10). CD8 T cells that expressed both Hobit and granzyme B, also contained high amounts of perforin (Fig. 8, C and D), suggesting that they have the machinery for immediate cytotoxicity. Interestingly, Hobit+ CD8 T cells that did not express granzyme B

contained perforin, although at lower levels than those that expressed granzyme B (Fig. 8, C and D). These cells expressed high amounts of granzyme K instead of granzyme B (Fig. 8, C and D), suggesting that Hobit identifies separate cytotoxic populations that express either granzyme B or K during quiescence.

Antigenic stimulation down-regulates Hobit expression in human CD8 T cells

To establish whether Hobit was expressed in cytotoxic CD8 T cells after antigenic stimulation, naive CD8 T cells were stimulated with anti-CD3/28 and IL-2 for 3 days and Hobit expression was analyzed. In contrast to Blimp-1, Hobit was not induced at the mRNA or protein level in naive CD8 T cells after TCR stimulation (Fig. 9, A-C). To address whether Hobit+ effector-type CD8 T cells maintained Hobit expression after activation, we stimulated the cells *in vitro* with anti-CD3/28 and IL-2. In contrast to Blimp-1, Hobit was strongly down-regulated in effector-type CD8 T cells after 3 days of stimulation with anti-CD3/28 and IL-2 (Fig. 9, A-C). To examine whether the down-regulation of Hobit was a direct effect of T cell activation, we briefly cultured effector-type CD8 T cells in the presence of PMA and ionomycin. Hobit mRNA was strongly down-regulated in effector-type CD8 T cells as early as 4 hours after activation with PMA and ionomycin (Fig. 9D). Hobit protein was also down-regulated in effector-type CD8 T cells after 4 hrs of PMA and ionomycin stimulation, but the down-regulation was not complete at this early time-point (Fig. 9, E and F). To determine whether the expression regulation of human Hobit was similar *in vivo*, we followed HCMV- and EBV-specific CD8 T cells over time after primary HCMV and EBV infection in kidney transplant recipients. HCMV-specific CD8 T cells (HCMV-TPR) and EBV-specific CD8 T cells (EBV-EPL) were divided into proliferating and non-proliferating cells using the proliferation-associated marker Ki67 and analyzed for Hobit expression (Fig. 9G). Ki67high CD8 T cells had

reduced expression of Hobit compared to Ki67low CD8 T cells (Fig. 9G), underlining that recent antigen encounter suppresses Hobit expression *in vivo*. Similar results were obtained in a longitudinal study of a second kidney transplant patient (unpublished observations). The expression regulation of Hobit resulted in strong overlap between Hobit and granzyme B expression under steady state conditions, but not after *in vitro* activation (Fig. 9H). In contrast, Blimp-1 protein was not co-expressed with granzyme B in peripheral blood CD8 T cells under resting conditions, but was induced in granzyme B+ cells after TCR stimulation (Fig. 9H). Thus, Hobit was specifically expressed in CD8 T cells with cytotoxic potential under resting conditions in contrast to Blimp-1 that was upregulated in cytotoxic CD8 T cells after activation. These findings suggest that Hobit and Blimp-1 may regulate granzyme B under similar conditions, but in different subsets of CD8 T cells in humans and mice.

Discussion:

In this report, we describe that the expression regulation of Hobit and Blimp-1 occurs in opposite directions during antigen-induced CD8 T cell differentiation. In CD8 T cells, Blimp-1 is up-regulated by activation, whereas Hobit is not. Blimp-1 mRNA, but not Blimp-1 protein, is maintained in long-lived effector-type and memory populations of CD8 T cells, indicating that Blimp-1 is repressed by post-transcriptional mechanisms in CD8 T cells. These findings suggested that Blimp-1 did not contribute to the persistence of cytotoxic functions in CD8 T cells at late time-points after infection. Indeed, we established that Hobit was an essential transcriptional regulator for the maintenance of granzyme B in CD8 T cells during the memory phase. In contrast to Blimp-1, Hobit is rapidly downregulated in antigen-experienced CD8 T cells after re-stimulation. Thus, the Hobit and Blimp-1-driven

transcriptional regulation of cytotoxicity appears temporally separated in CD8 T cells with an early role for Blimp-1 in primary effector cells and a late role for Hobit in memory cells.

The Blimp-1 GFP reporter has been a highly valuable tool in the assessment of the expression pattern of Blimp-1 in B and T lymphocytes (22,31). The reporter has been shown to truthfully reflect Blimp-1 expression at the mRNA level during B and T cell differentiation, but does not necessarily take into consideration the posttranscriptional regulation that may occur at the level of translation or at the level of proteasomal degradation. We have observed a discrepancy between the expression of Blimp-1 mRNA and protein during quiescence in memory CD8 T cells, suggesting that in these lymphocyte populations posttranscriptional regulation is relevant to acquire Blimp-1 protein. The mechanisms underlying posttranscriptional regulation of Blimp-1 are unclear. It is possible that sumoylation plays a role, as this process has previously been reported to target Blimp-1 for degradation by the proteasome (32). The expression of Blimp-1 protein has not been directly examined in other Blimp-1+ populations such as regulatory T cells and plasma cells. Functional analyses using conditional deletion of Blimp-1 suggest that Blimp-1 protein activity remains during quiescence in plasma cells, although such analyses do not rule out that more subtle differences in protein expression occur (33). As regulatory T cells and plasma cells in contrast to CD8 T cells do not up-regulate Hobit under homeostatic conditions, we speculate that persistence of Blimp-1 protein and acquisition of Hobit are alternative strategies of these separate lineages to maintain the Hobit/Blimp-1 transcriptional module during quiescence.

We have previously published that human Hobit is expressed in circulating populations of NK cells and antigen-experienced CD4 and CD8 T cells (20,34) in contrast to murine Hobit, which is specifically expressed in Trm and other resident lymphocytes including ILC1 and NKT cells (19). We speculate that divergent evolutionary pressures by distinct mouse and human pathogens may have driven the unique expression patterns of Hobit in mice and humans. In line with this reasoning, human CMV, which has a long history of co-evolution with the human species induces the formation of Hobit+ CD4 and CD8 T cells in the circulation (20,34). Hobit may be essential to drive persistent granzyme B-driven cytotoxicity in CMV-specific CD8 T cells to enable continuous patrol of the endothelium and to maintain latency of the CMV infection. Hobit does not appear to share the posttranscriptional regulation with Blimp-1, as the expression of Hobit mRNA perfectly aligned with Hobit protein within human CD8 T cells and NK cells (20). The late defect in granzyme B production in Trm of Hobit deficient mice also indicates persistent expression of murine Hobit at the protein level. Currently, the full spectrum of the signaling pathways acting upstream of Hobit expression are unknown. In line with expression during the resting phase, we have found that the homeostatic cytokine IL-15 is involved in the induction of Hobit expression in Trm (19). Consistent with an exclusive role during quiescence, we have shown that Hobit was downregulated within hours after T cell activation at both the mRNA and protein level. Indeed, Hobit is not found in short-lived effectors during primary infection, but is present in Temra and Trm cells that display direct effector function and that persist during quiescence (19,20). The rapid kinetics of the decrease in expression after triggering with PMA and ionomycin indicates direct involvement of TCR signaling pathways in Hobit downregulation. In contrast to Hobit, Blimp-1 appears to be induced in response to inflammatory signals. Blimp-1 expression markedly increases during effector differentiation

of CD8 T cells *in vivo* (22,23,27), and the transcription factor is also upregulated after antigenic stimulation in combination with cytokines such as IL-2, IL-12 and IL-21 *in vitro* (35-38). Similarly, human NK cells up-regulate Blimp-1 expression after stimulation *in vitro* with IL-12 and IL-18 (39). Blimp-1 expression may be self-limiting, given that the transcription factor can suppress its own expression (36). In support of a direct role for Blimp-1 in a negative feedback loop in the regulation of its expression, the Blimp-1 locus contains a binding site for Blimp-1, which is not present in the Hobit locus (19). These data are in line with transient expression of Blimp-1 and persistent expression of Hobit in the CD8 T cell lineage. The expression regulation suggests that despite the overlap in transcriptional targets, Hobit and Blimp-1 have non-redundant roles in immune regulation, as they are expressed under resting and inflammatory conditions, respectively.

Hobit and Blimp-1 are homologous transcription factors that display the highest degree of similarity in the Zinc Finger domains (18,20). This region in both Hobit and Blimp-1 is essential for the binding to "GAAAG"-containing DNA sequences, providing rationale for their highly overlapping direct target genes in CD8 T cells (19,20). Blimp-1 directly bound within the granzyme B locus, suggesting direct involvement in the transcriptional regulation of cytotoxicity (19). In contrast, we were unable to find evidence for direct binding of Hobit at these sites. Technical reasons relating to sensitivity may underlie the difference, as the total number of target genes was about ten-fold lower for Hobit than for Blimp-1 (19). Previously, we have shown in NKT cells that Hobit is involved in the regulation of granzyme B expression at the transcript level (18). Here, we have established an essential role for Hobit in the transcriptional regulation of granzyme B in Trm of liver and gut. As Blimp-1 similar to Hobit positively regulates granzyme B expression (22,23), it appears that both

factors instruct the same transcriptional program to establish cytotoxicity. At odds with the induction of granzyme B expression, Blimp-1 has been described as a transcriptional repressor that silences the expression of target genes through the recruitment of co-repressors including the histone H3K9 methyltransferase G9a, Groucho family proteins and histone deacetylases (40-42). However, similar to the positive role of Blimp1 in the induction of granzyme B expression, Blimp1 was also found to be required for the upregulation of IL-10 expression in regulatory T cells and Tr1 (43,44). Indeed. recently, it has become clear that during plasma cell differentiation Blimp-1 also associates with putative co-activators such as the chromatin-remodeling BAF complex to establish active histone marks in its target genes (45). The epigenetic landscape of the granzyme B locus has been studied in human and mouse circulating memory cells and evidence for the presence of active hyperacytylation at H3K9 and the absence of repressive hypermethylation at H3K27 has been found (14,15). At this stage it is unclear whether these epigenetic marks are preserved in Trm and Temra cells or whether these cells contain unique epigenetic marks. Thus, our findings suggest that Blimp-1 contributes to the transcriptional regulation of cytotoxicity during an infection and Hobit after clearance of infection, but the potential role of these transcription factors in the establishment of these epigenetic marks remains unexplored.

In contrast to Trm that are formed in liver and gut after LCMV infection, Trm that develop in skin after HSV-1 infection and in lungs after infection with respiratory viruses do not express granzyme B protein (46,47). As HSV-1-specific Trm within the skin maintain higher expression of granzyme B mRNA than circulating memory populations (47), it appears that these Trm also display improved retention of cytotoxic capacity, although not at the level of granzyme B protein expression. The differences in the maintenance of granzyme B

expression between Trm populations may relate to tissue-specific adaptations that arise between Trm located at different sites. In support of tissue-specific regulation of granzyme B expression, Trm within the dorsal root ganglia that co-arise with skin-resident Trm after infection with HSV-1 express granzyme B at the protein level (47). As Hobit is expressed in Trm throughout tissues (19), Hobit expression does not appear to be sufficient for the induction of granzyme B protein in all of these Trm populations.

Long-lived CD8 T cells with direct cytotoxic potential are superior compared to other memory cells in that these cells are able to respond directly without the need of proliferation and differentiation, which enables them to mount immune responses at an accelerated pace. Here, we have identified that Hobit rather than Blimp-1 is an essential transcriptional regulator in the long-term maintenance of granzyme B-driven cytotoxicity of memory CD8 T cells. Other transcription factors such as T-bet, Eomes, Runx-3 and Notch, which have all been shown to establish cytotoxicity in effector CD8 T cells through the induction of granzyme B and or perforin (25,48,49), may contribute to the regulation of cytotoxicity in memory cells. In contrast to Hobit, these transcription factors are not exclusively expressed in memory cells with direct cytotoxic potential, suggesting that they do not have a specific role in the long-term maintenance of cytotoxicity. Moreover, T-bet and Eomes are downregulated in granzyme B+ Trm populations compared to granzyme B- circulating memory populations (50). Thus, our findings have established a Hobit-driven transcriptional network underlying the maintenance of cytotoxicity in CD8 T cells that may provide essential clues to the future use of memory cells with immediate killing capacity in adoptive therapies in patients.

Material and Methods:

Human material

Human PBMCs were obtained from fresh heparinized blood or buffy coats of healthy donors using Ficoll-Paque Plus (GE Healthcare) gradient centrifugation. Total, naive, effector and memory CD8+ T cells were isolated using magnetic sorting with CD8 microbeads (Miltenyi Biotec) and then flow-cytometric sorting for CD27 and CD45RA on a FACS Aria (BD Biosciences) to obtain CD27+CD45RA+ naive, CD27-CD45RA+ effector and CD27+CD45RA- memory cells. We have used blood samples from a kidney transplant patient who was EBV and hCMV seronegative before transplant and who underwent a primary EBV and hCMV infection after receipt of a kidney from a EBV+ and hCMV+ donor. The patient received an immunosuppressive regimen that included prednisolone, cyclosporine A and mycophenolate mofetil. All donors gave written informed consent prior to inclusion in the study and the study was approved by the Amsterdam Medical Center institutional medical ethics committee.

Mice

WT, *Zfp683*$^{-/-}$ (*Hobit* KO) (18) and *Prdm1*$^{flox/flox}$ x Lck Cre (*Blimp-1* KO) mice (22) were maintained on a C57Bl/6 background. Mice were bred under SPF conditions and animal experiments were performed according to national and institutional guidelines.

Antibodies

The following anti-mouse monoclonal antibodies for flow cytometry were purchased from eBioscience, BD Biosciences, Invitrogen or Biolegend: anti-CD3 (145-2C11), anti-TCRβ (H57-

597), anti-CD4 (RM4-5, GK1.5, and MT4), anti-CD8 (53-6.7), anti-CD44 (IM7), anti-CD62L (MEL-14), anti-CD69 (H1.2F3), anti-Ly5.1 (A20), anti-Ly5.2 (104), anti-IFN-γ (XMG1.2), anti-Trail (N2B2), anti-granzyme B (GB-11) and anti-Fas ligand (MFL3). The following anti-human monoclonal antibodies for flow cytometry were purchased from Sanquin Reagents, eBioscience and BD Biosciences: anti-CD8 (RPA-T8), anti-CD27 (O323), anti-CD45RA (HI100) and anti-CD3 (SK7). Antibodies against human Hobit (Sanquin-Hobit/1) were made in house, as previously described (20). The following antibodies were used for western blotting: anti-Blimp-1 (6D3; eBioscience), anti-β-actin (AC-15; Sigma-Aldrich) and conjugated goat anti-mouse secondary antibodies (DAKO).

Tetramers

To detect LCMV-specific CD8 T cells, MHC class I D^b restricted tetramers for the viral epitopes GP_{33-41} and $NP_{396-404}$ were produced as described (51). To detect NKT cells, tetramers of CD1d containing the α-GalCer derivative PBS57 were obtained from the Tetramer Core Facility of the US National Institutes of Health.

LCMV infection

Mice were infected intraperitoneally with 30 plague-forming units (PFU) of the LCMV strain WE or with 1×10^5 PFU of the LCMV strain Armstrong. At the indicated time points after infection mice were sacrificed and organs were collected for analysis of CD8 T cell responses.

***In vivo* NKT cell activation**

Mice were injected intraperitoneally with 2 μg α-galactosylceramide (KRN7000; Enzo Life Sciences) in 200 μl PBS to specifically activate NKT cells in an antigen-dependent manner. At various time points after immunization, mice were sacrificed and organs were collected for analysis of the activated NKT cells.

Cell preparation from murine tissues

Spleen and liver were isolated and ground over 70 μM nylon cell strainers (BD Biosciences) to obtain single-cell suspensions in PBS containing 0.5% BSA. Liver lymphocytes were separated from the other cell fractions via Percoll (GE Healthcare) gradient centrifugation. Liver-cell preparations were resuspended in 44% Percoll solution and pelleted lymphocyte-enriched fractions were collected after centrifugation. Erythrocytes in spleen and liver cell suspensions were lysed (155 mM NH_4Cl, 10 mM $KHCO_3$ and 1 mM EDTA) for removal of red blood cells. For the isolation of intraepthelial lymphocytes (IELs) the small intestine was cleared of fat tissue, Peyer's patches, and fecal content. Then, 1 cm^2 pieces of small intestine were incubated for 30 minutes at 37°C in Ca^{2+} and Mg^{2+} Free Hank's buffer (Gibco) containing 5 mM EDTA and 1 mM DTT. IELs were separated from the other cell fractions via density gradient centrifugation using 44% and 66% Percoll that enable enrichment of IELs at the interface of these layers. Cells were counted with an automated cell counter (CaseyCounter (Innovatis)).

***In vitro* CD8 T cell stimulation**

Human CD8 T cells were activated in 24 or 96-wells plates (Costar) coated with 3.5 μg/ml goat anti-mouse IgG antibodies (Jackson Immunoresearch) and 5 μg/ml anti-CD3 (HIT3a;

eBioscience) in the presence of 1 μg/ml anti-CD28 (CD28.2; eBioscience) and 50 U/ ml IL-2 (Peprotech) for the indicated time. For short-term activation, CD8 T cells were cultured with PMA (2 ng/ml; Sigma-Aldrich) and ionomycin (1 μg/ml; Sigma-Aldrich) for 4 hours. For the degranulation assay, LCMV-specific CD8 T cells were activated in 24 wells plates in the presence of 5 μg/ml GP_{33-41} and incubated for 4 hours in the presence of CD107a antibodies (eBio1D43; eBioscience). Brefeldin A (eBioscience) and Monensin (eBioscience) were added to enable intracellular capture of IFN-γ. For the cytotoxicity assay, CD8 T cells were isolated from the liver of LCMV immune mice that had received anti-ARTC2 nanobodies (BioLegend) directly prior to sacrifice. The anti-ARTC2 nanobodies were used to maintain the viability of the isolated CD8 T cells during culture. The isolated CD8 T cells were incubated with EL-4 cells that were labeled with Cell Trace Violet (Thermo Fisher Scientific) according to the manufacturer's protocol and loaded with 5 μg/ml GP_{33-41} peptide. The percentage of killing was measured using the viability dye Near-IR (Thermo Fisher Scientific) as a readout.

***In vitro* NKT cell stimulation**

NKT cells were enriched from single cell preparations of thymus using magnetic depletion of CD8+ and CD24+ thymocytes with anti-CD8 and anti-CD24 antibodies and goat anti-rat beads (Qiagen) and subsequent cell sorting with anti-TCRβ antibodies and PBS57-loaded CD1d tetramers. Isolated NKT cells were stimulated with plate-bound anti-CD3 antibodies (5 μg/ml) in medium containing anti-CD28 (2 μg/ml) and IL-2 (100 U/ml). Expanded NKT cells were re-plated after 3 days in medium containing IL-15 (20 ng/ml) and cultured for an additional 2 to 6 days. For adoptive transfer experiments with NKT cells, *in vitro* expanded NKT cells (1 x 10^6 cells) were transferred by intravenous injection. Recipient mice were sacrificed at the indicated time points for analysis of donor NKT cells.

PCR and quantitative PCR

RNA was isolated using Trizol Reagent (Invitrogen). cDNA synthesis was performed on a Verity 96 wells Fast Thermo Cycler (Applied Biosystems) using the iScript RT PCR kit (Biorad). Quantitative PCR was performed on a StepOnePlus system (Applied Biosystems) using the FAST SybrGreen mix (Life Technologies). The following primersets were used: murine Hobit (forward: 5'-TCCTCCCACTCTCATCTCCAA-3', reverse: 5'-CAGACCCACTGGCTGTCAT-3'), murine Blimp-1 (forward: 5'-GACGGGGGTACTTCTGTTCA-3', reverse: 5'-GGCATTCTTGGGAACTGTGT-3') granzyme B (forward: 5'-AAACGTGCTTCCTTTCGGG-3', reverse: 5'-GAAACTATGCCTGCAGCCACT-3'), HPRT (forward: 5'-TGAAGAGCTACTGTAATGATCAGTCAAC-3', reverse: 5'-AGCAAGCTTGCAACCTTAACCA-3'), Perforin (forward: 5'-GCAGCTGAGAAGACCTATCAGGAC-3', reverse: 5'-TCTGAGCGCCTTTTTGAAGTC-3'), human Hobit (forward: 5'-CATATGTGGCAAGAGCTTTGG-3', reverse: 5'-GGCAAGTTGAGTGAAGCTCT-3', human Blimp-1 (forward: 5'-GTGTCAGAACGGGATGAACA-3', reverse: 5'-GCTCGGTTGCTTTAGACTGC-3'), 18S (forward: 5'-GGACAACAAGCTCCGTGAAGA-3', reverse: 5'-CAGAAGTGACGCAGCCCTCTA-3'). Values are represented relative to that of 18S or HPRT and calibrated relative to naive CD8 T cells unless indicated otherwise.

RNA sequencing

RNA sequencing data was obtained from LCMV specific CD8 T cell subsets at day 40+ post infection using gp33 and np396 tetramers, as described (19). From this dataset, genes involved in cytotoxicity were selected for comparison of their expression profile in the indicated LCMV specific CD8+ memory T cell subsets.

Flow cytometry

Cells were stained for 30 min at 4°C with fluorochrome-conjugated antibodies in PBS 0.5% BSA. Intracellular stainings were performed after fixation and permeabilization with the FoxP3 transcription factor staining set (eBioscience) or with the cytofix/cytoperm kit (BD Biosciences). Tetramer labeling was performed at 4°C. Samples were measured with an LSR Fortessa or a Canto II flow cytometer (BD Biosciences) and expression was analyzed using FlowJo software (Tree Star). We have adhered to previously published flow cytometry guidelines (52).

Western Blotting

Cells were lysed in buffer containing 2% SDS, 66 mM Tris pH 7, 4 % β-mercaptoethanol and 1% protease inhibitor (Calbiochem). Proteins were separated on a NuPAGE 4-12% Bis-Tris gel (Novex, Life Technologies), after which proteins were transferred onto an iBlot Nitrocellulose Gel Transfer Stack (Novex, Life Technologies) using an iBlot or iBlot 2 (Life Technologies). Membranes were stained using the Pierce ECL Western Blot substrate kit (Life Technologies) and proteins were visualized on Fuji Medical X-ray Film using a Medical Film Processor (Konica Minolta Medical & Graphic. Inc, SRX-101A).

Statistics

Values are expressed as mean + SD or SEM as indicated. Differences between two groups were assessed by Student's t test. Differences between more than two groups were assessed using one-way ANOVA followed by a Bonferroni post-hoc test. A p-value of less than 0.05 was considered statistically significant (* $p<0.05$; ** $p<0.01$; *** $p<0.001$).

Acknowledgements:

RS and PH are supported by Veni fellowships from The Netherlands Organisation for Health Research and Development (ZonMW). FMB and KPJMvG are supported by a Vidi fellowship from ZonMW. KPJMvG is also supported by a fellowship from the Landsteiner Foundation for Blood Transfusion Research (LSBR).

Conflict of interest:

The authors declare no financial or commercial conflict of interest

References:

1. Kagi, D., F. Vignaux, B. Ledermann, K. Burki, V. Depraetere, S. Nagata, H. Hengartner, and P. Golstein. 1994. Fas and perforin pathways as major mechanisms of T cell-mediated cytotoxicity. *Science* 265: 528-530.
2. Lowin, B., M. Hahne, C. Mattmann, and J. Tschopp. 1994. Cytolytic T-cell cytotoxicity is mediated through perforin and Fas lytic pathways. *Nature* 370: 650-652.
3. Voskoboinik, I., J. C. Whisstock, and J. A. Trapani. 2015. Perforin and granzymes: function, dysfunction and human pathology. *Nat. Rev. Immunol.* 15: 388-400.
4. Kagi, D., B. Ledermann, K. Burki, P. Seiler, B. Odermatt, K. J. Olsen, E. R. Podack, R. M. Zinkernagel, and H. Hengartner. 1994. Cytotoxicity mediated by T cells and natural killer cells is greatly impaired in perforin-deficient mice. *Nature* 369: 31-37.
5. Smyth, M. J., K. Y. Thia, S. E. Street, D. Macgregor, D. I. Godfrey, and J. A. Trapani. 2000. Perforin-mediated cytotoxicity is critical for surveillance of spontaneous lymphoma. *J. Exp. Med.* 192: 755-760.

6. Chowdhury, D., and J. Lieberman. 2008. Death by a thousand cuts: granzyme pathways of programmed cell death. *Annu. Rev. Immunol.* 26: 389-420.
7. Hamann, D., P. A. Baars, M. H. Rep, B. Hooibrink, S. R. Kerkhof-Garde, M. R. Klein, and R. A. van Lier. 1997. Phenotypic and functional separation of memory and effector human CD8+ T cells. *J. Exp. Med.* 186: 1407-1418.
8. Sallusto, F., D. Lenig, R. Forster, M. Lipp, and A. Lanzavecchia. 1999. Two subsets of memory T lymphocytes with distinct homing potentials and effector functions. *Nature* 401: 708-712.
9. Sathaliyawala, T., M. Kubota, N. Yudanin, D. Turner, P. Camp, J. J. Thome, K. L. Bickham, H. Lerner, M. Goldstein, M. Sykes, T. Kato, and D. L. Farber. 2013. Distribution and compartmentalization of human circulating and tissue-resident memory T cell subsets. *Immunity.* 38: 187-197.
10. Ariotti, S., M. A. Hogenbirk, F. E. Dijkgraaf, L. L. Visser, M. E. Hoekstra, J. Y. Song, H. Jacobs, J. B. Haanen, and T. N. Schumacher. 2014. T cell memory. Skin-resident memory CD8(+) T cells trigger a state of tissue-wide pathogen alert. *Science* 346: 101-105.
11. Schenkel, J. M., K. A. Fraser, V. Vezys, and D. Masopust. 2013. Sensing and alarm function of resident memory CD8(+) T cells. *Nat. Immunol.* 14: 509-513.
12. Schenkel, J. M., K. A. Fraser, L. K. Beura, K. E. Pauken, V. Vezys, and D. Masopust. 2014. T cell memory. Resident memory CD8 T cells trigger protective innate and adaptive immune responses. *Science* 346: 98-101.
13. Wolint, P., M. R. Betts, R. A. Koup, and A. Oxenius. 2004. Immediate cytotoxicity but not degranulation distinguishes effector and memory subsets of CD8+ T cells. *J. Exp. Med.* 199: 925-936.

14. Araki, Y., M. Fann, R. Wersto, and N. P. Weng. 2008. Histone acetylation facilitates rapid and robust memory CD8 T cell response through differential expression of effector molecules (eomesodermin and its targets: perforin and granzyme B). *J. Immunol.* 180: 8102-8108.

15. Zediak, V. P., J. B. Johnnidis, E. J. Wherry, and S. L. Berger. 2011. Cutting edge: persistently open chromatin at effector gene loci in resting memory CD8+ T cells independent of transcriptional status. *J. Immunol.* 186: 2705-2709.

16. Masopust, D., V. Vezys, E. J. Wherry, D. L. Barber, and R. Ahmed. 2006. Cutting edge: gut microenvironment promotes differentiation of a unique memory CD8 T cell population. *J. Immunol.* 176: 2079-2083.

17. Steinbach, K., I. Vincenti, M. Kreutzfeldt, N. Page, A. Muschaweckh, I. Wagner, I. Drexler, D. Pinschewer, T. Korn, and D. Merkler. 2016. Brain-resident memory T cells represent an autonomous cytotoxic barrier to viral infection. *J. Exp. Med.* 213: 1571-1587.

18. van Gisbergen, K. P., N. A. Kragten, K. M. Hertoghs, F. M. Wensveen, S. Jonjic, J. Hamann, M. A. Nolte, and R. A. van Lier. 2012. Mouse Hobit is a homolog of the transcriptional repressor Blimp-1 that regulates NKT cell effector differentiation. *Nat. Immunol.* 13: 864-871.

19. Mackay, L. K., M. Minnich, N. A. Kragten, Y. Liao, B. Nota, C. Seillet, A. Zaid, K. Man, S. Preston, D. Freestone, A. Braun, E. Wynne-Jones, F. M. Behr, R. Stark, D. G. Pellicci, D. I. Godfrey, G. T. Belz, M. Pellegrini, T. Gebhardt, M. Busslinger, W. Shi, F. R. Carbone, R. A. van Lier, A. Kallies, and K. P. van Gisbergen. 2016. Hobit and Blimp1 instruct a universal transcriptional program of tissue residency in lymphocytes. *Science* 352: 459-463.

20. Vieira Braga, F. A., K. M. Hertoghs, N. A. Kragten, G. M. Doody, N. A. Barnes, E. B. Remmerswaal, C. C. Hsiao, P. D. Moerland, D. Wouters, I. A. Derks, S. A. van, M. Demkes, J. Hamann, E. Eldering, M. A. Nolte, R. M. Tooze, I. J. Ten Berge, K. P. van Gisbergen, and R. A. van Lier. 2015. Blimp-1 homolog Hobit identifies effector-type lymphocytes in humans. *Eur. J. Immunol.*

21. Kallies, A., and S. L. Nutt. 2007. Terminal differentiation of lymphocytes depends on Blimp-1. *Curr. Opin. Immunol.* 19: 156-162.

22. Kallies, A., A. Xin, G. T. Belz, and S. L. Nutt. 2009. Blimp-1 transcription factor is required for the differentiation of effector CD8(+) T cells and memory responses. *Immunity.* 31: 283-295.

23. Rutishauser, R. L., G. A. Martins, S. Kalachikov, A. Chandele, I. A. Parish, E. Meffre, J. Jacob, K. Calame, and S. M. Kaech. 2009. Transcriptional repressor Blimp-1 promotes CD8(+) T cell terminal differentiation and represses the acquisition of central memory T cell properties. *Immunity.* 31: 296-308.

24. Xin, A., F. Masson, Y. Liao, S. Preston, T. Guan, R. Gloury, M. Olshansky, J. X. Lin, P. Li, T. P. Speed, G. K. Smyth, M. Ernst, W. J. Leonard, M. Pellegrini, S. M. Kaech, S. L. Nutt, W. Shi, G. T. Belz, and A. Kallies. 2016. A molecular threshold for effector CD8(+) T cell differentiation controlled by transcription factors Blimp-1 and T-bet. *Nat. Immunol.* 17: 422-432.

25. Backer, R. A., C. Helbig, R. Gentek, A. Kent, B. J. Laidlaw, C. X. Dominguez, Y. S. de Souza, S. E. van Trierum, B. R. van, G. F. Rimmelzwaan, B. A. ten, A. M. Willemsen, A. H. van Kampen, S. M. Kaech, J. M. Blander, G. K. van, and D. Amsen. 2014. A central role for Notch in effector CD8(+) T cell differentiation. *Nat. Immunol.* 15: 1143-1151.

26. Joshi, N. S., W. Cui, A. Chandele, H. K. Lee, D. R. Urso, J. Hagman, L. Gapin, and S. M. Kaech. 2007. Inflammation directs memory precursor and short-lived effector CD8(+) T cell fates via the graded expression of T-bet transcription factor. *Immunity.* 27: 281-295.

27. Shin, H., S. D. Blackburn, A. M. Intlekofer, C. Kao, J. M. Angelosanto, S. L. Reiner, and E. J. Wherry. 2009. A role for the transcriptional repressor Blimp-1 in CD8(+) T cell exhaustion during chronic viral infection. *Immunity.* 31: 309-320.

28. Kallies, A., S. Carotta, N. D. Huntington, N. J. Bernard, D. M. Tarlinton, M. J. Smyth, and S. L. Nutt. 2011. A role for Blimp1 in the transcriptional network controlling natural killer cell maturation. *Blood* 117: 1869-1879.

29. Appay, V., P. R. Dunbar, M. Callan, P. Klenerman, G. M. Gillespie, L. Papagno, G. S. Ogg, A. King, F. Lechner, C. A. Spina, S. Little, D. V. Havlir, D. D. Richman, N. Gruener, G. Pape, A. Waters, P. Easterbrook, M. Salio, V. Cerundolo, A. J. McMichael, and S. L. Rowland-Jones. 2002. Memory CD8+ T cells vary in differentiation phenotype in different persistent virus infections. *Nat. Med.* 8: 379-385.

30. Hertoghs, K. M., P. D. Moerland, S. A. van, E. B. Remmerswaal, S. L. Yong, P. J. van de Berg, S. M. van Ham, F. Baas, I. J. Ten Berge, and R. A. van Lier. 2010. Molecular profiling of cytomegalovirus-induced human CD8+ T cell differentiation. *J. Clin. Invest* 120: 4077-4090.

31. Kallies, A., J. Hasbold, D. M. Tarlinton, W. Dietrich, L. M. Corcoran, P. D. Hodgkin, and S. L. Nutt. 2004. Plasma cell ontogeny defined by quantitative changes in blimp-1 expression. *J. Exp. Med.* 200: 967-977.

32. Ying, H. Y., S. T. Su, P. H. Hsu, C. C. Chang, I. Y. Lin, Y. H. Tseng, M. D. Tsai, H. M. Shih, and K. I. Lin. 2012. SUMOylation of Blimp-1 is critical for plasma cell differentiation. *EMBO Rep.* 13: 631-637.

33. Tellier, J., W. Shi, M. Minnich, Y. Liao, S. Crawford, G. K. Smyth, A. Kallies, M. Busslinger, and S. L. Nutt. 2016. Blimp-1 controls plasma cell function through the regulation of immunoglobulin secretion and the unfolded protein response. *Nat. Immunol.* 17: 323-330.

34. Oja, A. E., F. A. Vieira Braga, E. B. Remmerswaal, N. A. Kragten, K. M. Hertoghs, J. Zuo, P. A. Moss, R. A. van Lier, K. P. van Gisbergen, and P. Hombrink. 2017. The Transcription Factor Hobit Identifies Human Cytotoxic CD4(+) T Cells. *Front Immunol.* 8: 325.

35. Cimmino, L., G. A. Martins, J. Liao, E. Magnusdottir, G. Grunig, R. K. Perez, and K. L. Calame. 2008. Blimp-1 attenuates Th1 differentiation by repression of ifng, tbx21, and bcl6 gene expression. *J. Immunol.* 181: 2338-2347.

36. Gong, D., and T. R. Malek. 2007. Cytokine-dependent Blimp-1 expression in activated T cells inhibits IL-2 production. *J. Immunol.* 178: 242-252.

37. Martins, G. A., L. Cimmino, J. Liao, E. Magnusdottir, and K. Calame. 2008. Blimp-1 directly represses Il2 and the Il2 activator Fos, attenuating T cell proliferation and survival. *J. Exp. Med.* 205: 1959-1965.

38. Salehi, S., R. Bankoti, L. Benevides, J. Willen, M. Couse, J. S. Silva, D. Dhall, E. Meffre, S. Targan, and G. A. Martins. 2012. B lymphocyte-induced maturation protein-1 contributes to intestinal mucosa homeostasis by limiting the number of IL-17-producing CD4+ T cells. *J. Immunol.* 189: 5682-5693.

39. Smith, M. A., M. Maurin, H. I. Cho, B. Becknell, A. G. Freud, J. Yu, S. Wei, J. Djeu, E. Celis, M. A. Caligiuri, and K. L. Wright. 2010. PRDM1/Blimp-1 controls effector cytokine production in human NK cells. *J. Immunol.* 185: 6058-6067.

40. Gyory, I., J. Wu, G. Fejer, E. Seto, and K. L. Wright. 2004. PRDI-BF1 recruits the histone H3 methyltransferase G9a in transcriptional silencing. *Nat. Immunol.* 5: 299-308.

41. Ren, B., K. J. Chee, T. H. Kim, and T. Maniatis. 1999. PRDI-BF1/Blimp-1 repression is mediated by corepressors of the Groucho family of proteins. *Genes Dev.* 13: 125-137.

42. Yu, J., C. Angelin-Duclos, J. Greenwood, J. Liao, and K. Calame. 2000. Transcriptional repression by blimp-1 (PRDI-BF1) involves recruitment of histone deacetylase. *Mol. Cell Biol.* 20: 2592-2603.

43. Cretney, E., A. Xin, W. Shi, M. Minnich, F. Masson, M. Miasari, G. T. Belz, G. K. Smyth, M. Busslinger, S. L. Nutt, and A. Kallies. 2011. The transcription factors Blimp-1 and IRF4 jointly control the differentiation and function of effector regulatory T cells. *Nat. Immunol.* 12: 304-311.

44. Heinemann, C., S. Heink, F. Petermann, A. Vasanthakumar, V. Rothhammer, E. Doorduijn, M. Mitsdoerffer, C. Sie, C. O. Prazeres da, T. Buch, B. Hemmer, M. Oukka, A. Kallies, and T. Korn. 2014. IL-27 and IL-12 oppose pro-inflammatory IL-23 in CD4+ T cells by inducing Blimp1. *Nat. Commun.* 5: 3770.

45. Minnich, M., H. Tagoh, P. Bonelt, E. Axelsson, M. Fischer, B. Cebolla, A. Tarakhovsky, S. L. Nutt, M. Jaritz, and M. Busslinger. 2016. Multifunctional role of the transcription factor Blimp-1 in coordinating plasma cell differentiation. *Nat. Immunol.* 17: 331-343.

46. Kohlmeier, J. E., T. Cookenham, A. D. Roberts, S. C. Miller, and D. L. Woodland. 2010. Type I interferons regulate cytolytic activity of memory CD8(+) T cells in the lung airways during respiratory virus challenge. *Immunity.* 33: 96-105.

47. Mintern, J. D., C. Guillonneau, F. R. Carbone, P. C. Doherty, and S. J. Turner. 2007. Cutting edge: Tissue-resident memory CTL down-regulate cytolytic molecule expression following virus clearance. *J. Immunol.* 179: 7220-7224.

48. Cruz-Guilloty, F., M. E. Pipkin, I. M. Djuretic, D. Levanon, J. Lotem, M. G. Lichtenheld, Y. Groner, and A. Rao. 2009. Runx3 and T-box proteins cooperate to establish the transcriptional program of effector CTLs. *J. Exp. Med.* 206: 51-59.

49. Pearce, E. L., A. C. Mullen, G. A. Martins, C. M. Krawczyk, A. S. Hutchins, V. P. Zediak, M. Banica, C. B. DiCioccio, D. A. Gross, C. A. Mao, H. Shen, N. Cereb, S. Y. Yang, T. Lindsten, J. Rossant, C. A. Hunter, and S. L. Reiner. 2003. Control of effector CD8+ T cell function by the transcription factor Eomesodermin. *Science* 302: 1041-1043.

50. Mackay, L. K., E. Wynne-Jones, D. Freestone, D. G. Pellicci, L. A. Mielke, D. M. Newman, A. Braun, F. Masson, A. Kallies, G. T. Belz, and F. R. Carbone. 2015. T-box transcription factors combine with the cytokines TGF-beta and IL-15 to control tissue-resident memory T cell fate. *Immunity.* 43: 1101-1111.

51. Altman, J. D., P. A. Moss, P. J. Goulder, D. H. Barouch, M. G. McHeyzer-Williams, J. I. Bell, A. J. McMichael, and M. M. Davis. 1996. Phenotypic analysis of antigen-specific T lymphocytes. *Science* 274: 94-96.

52. Cossarizza, A., Chang, H.D., Radbruch, A., Andrä, I, Annunziato, F., Bacher, P., Barnaba, V. et al., 2017. Guidelines for the use of flow cytometry and cell sorting in immunological studies *Eur. J. Immunol.* 47: 1584–1797.

Figure Legends:

Figure 1: Trm specifically upregulate cytotoxic molecules to maintain immediate cytotoxic potential. (A,B) The killing of peptide-loaded (closed triangles) and unloaded EL4 target cells (open triangles) was analyzed by flow cytometry at (A) 4 and (B) 24 hours of co-culture in the indicated effector/target ratios with virus-specific Tem (blue, left panels) or Trm (red, right panels) of LCMV-infected mice. Total CD62L-CD69- CD8 T cells (Tem) and CD62L-CD69+ (Trm) fractions of CD8 T cells at day 37 of infection were taken from liver of WT mice for use as effectors in the killing assays. EL (C) Heatmap displays the expression of the indicated cytotoxicity-associated genes (z-scores) in virus-specific circulating (Tcm and Tem) and resident memory CD8 T cells (Trm) of WT mice after infection with LCMV, as determined using RNA sequencing. Z-scores are color-coded, as indicated by legend. (D-F) The expression of granzyme B was analyzed by flow cytometry in virus-specific CD69-CD62L- (T effector or Tem) and CD69+CD62L- CD8 T cells (Trm) in spleen, liver and gut of WT mice at day 8 and day 33 after infection with LCMV-WE or day 49 LCMV-Armstrong, as indicated. (D) Histograms depict expression of granzyme B in the indicated populations of CD8 T cells. (E) The percentage of granzyme B+ T effector, Tem and Trm from the spleen, liver and small intestine (SI) after LCMV WE infection was quantified by flow cytometry. Data in (F) shows the quantification of the percentage of granzyme B+ Tem and Trm in spleen, liver and SI after LCMV Armstrong infection. (G,H) Histograms display expression of (G) Fas ligand and (H) Trail in virus-specific Tem and Trm within the liver of WT mice at day 61 after infection with LCMV. For comparison, TRAIL expression was analyzed in circulating (cNK) and tissue-resident NK cells (trNK) of the liver. Data in (A) displays results of seven mice from two pooled experiments and data in (B) displays data of two mice from one representative

experiment out of two experiments. Data in (D) displays representative examples from data in (E and F). Data in (E and F) displays the results from one representative experiment out of two with three or four mice per group. Data in (G and H) is representative of five to eight mice from two independent experiments. Data are shown as mean + SEM; ** $p<0.01$; *** $p < 0.001$, one-way ANOVA.

Kragten et al. Figure 1

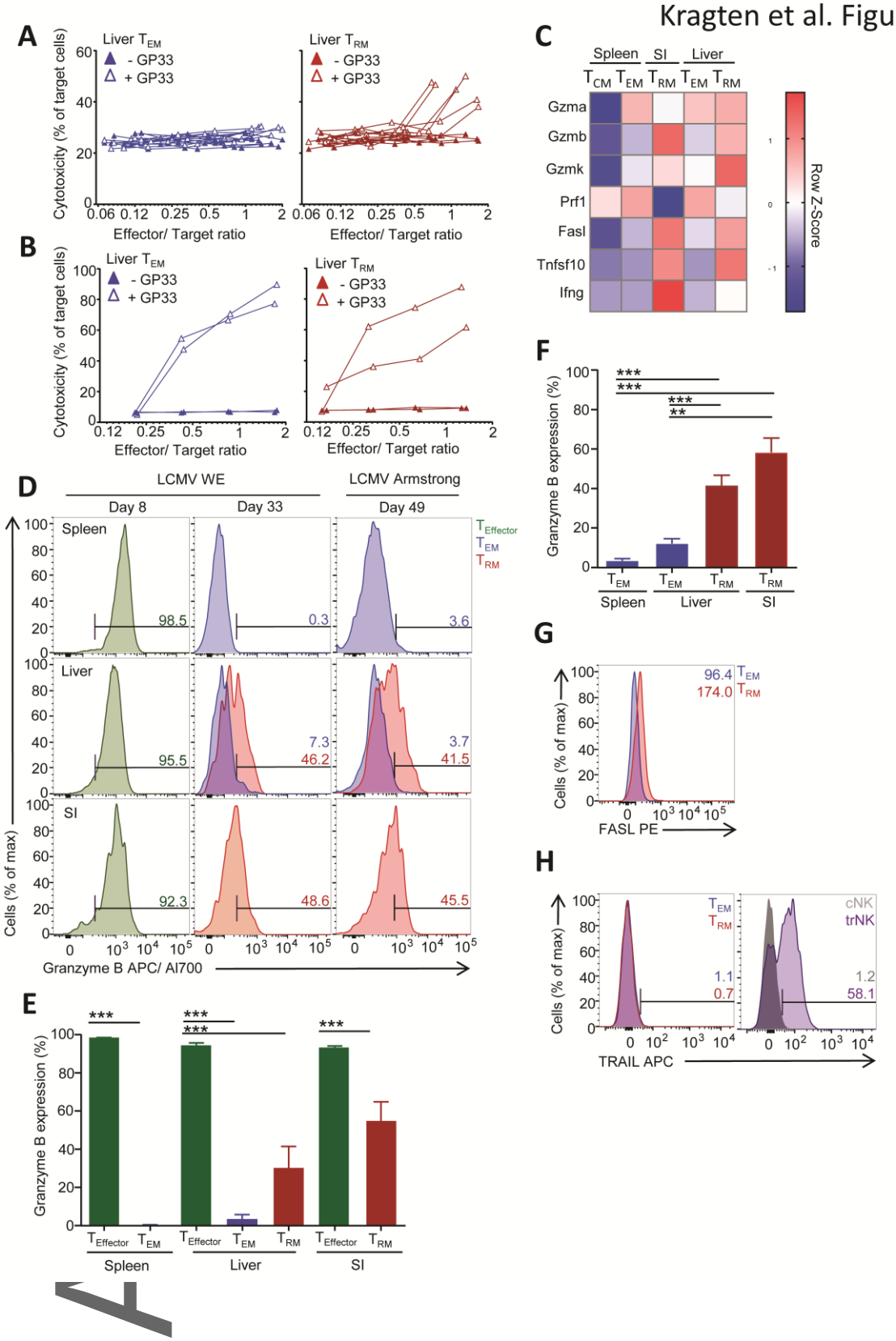

Figure 2: Blimp-1 regulates granzyme B expression after activation. The expression of granzyme B was analyzed by flow cytometry in virus-specific CD8 T cells of WT and *Blimp-1* KO mice at (A,B) day 8 and (C,D) day 36 after infection with LCMV Armstrong. (A) Contour plots display the expression of CD69 and granzyme B on gp33 tetramer+ effector CD8 T cells (in green) in spleen, liver and the intraepithelial fraction of small intestine (SI). (B) The percentage of LCMV-specific CD8 T cells that express granzyme B was quantified. (C) The expression of CD69 and granzyme B of gp33 tetramer+ effector memory (Tem; in blue) and tissue-resident memory (Trm; in red) is shown in representative contour plots. (D) The expression of granzyme B was quantified as a percentage of the indicated virus-specific memory CD8 T cells. Contour plots in (A, C) display representative results from data in (B, D), respectively. Data in (B) displays results of at least 5 mice per group from one representative experiment out of two independent experiments. Data in (D) displays results of at least 6 mice per group from two pooled experiments. Data are shown as mean + SEM; *** $p<0.001$, one-way ANOVA.

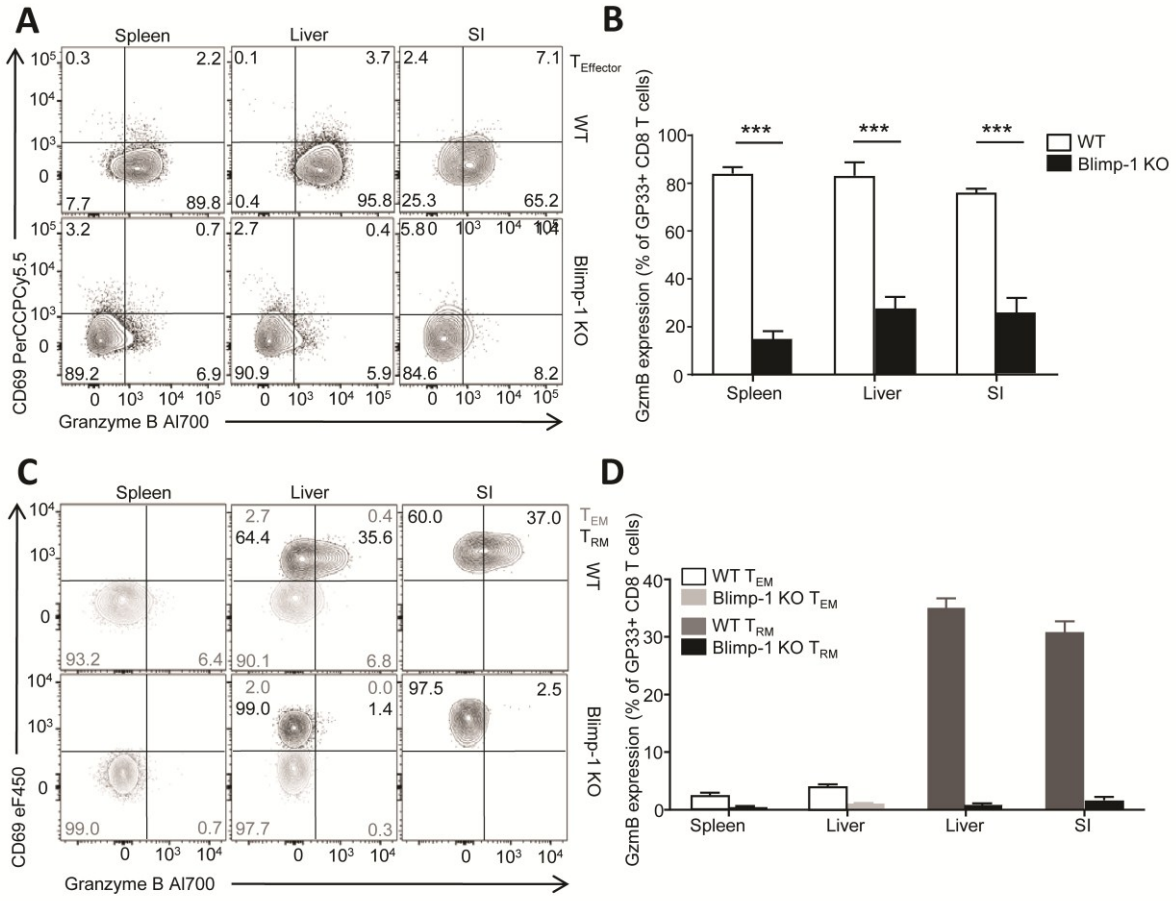

Figure 3: In mice, Blimp-1 protein is highly expressed in effector CD8 T cells, but not or at low levels in memory CD8 T cells. (A) The expression of Blimp-1 mRNA was analyzed using qPCR in the indicated subsets of virus-specific effector and memory CD8 T cells after LCMV Armstrong infection. (B-K) The expression of Blimp-1 protein was analyzed using flow cytometry in (B, C) plasma cells (PC), in (D-G) virus-specific effector CD8 T cells and in (H-K) virus-specific memory CD8 T cells at day 42 after LCMV Armstrong infection. (B, D, F, H, J) Histograms display expression of Blimp-1 in the indicated populations of Ly5.1+ or Ly5.1/2+ lymphocytes (yellow, plasma cells (PC); orange, T naive; green, T effector; purple, Tcm; blue, Tem; red, Trm). For reference, the expression of Blimp-1 was analyzed in congenically marked Ly5.2+ naive CD8 T cells (control; filled grey) that were added to all of the analyzed samples. (C, E, G, I, K) Bar graphs display the expression of Blimp-1 as a percentage of the indicated population. Histograms in (B, D, F, H, J) display representative results from data in (C, E, G, I, K), respectively. Data in (A, C, E, G, I, K) display results of four or five mice from one representative experiment out of at least two independent experiments. Data are shown as mean + SD; ** $p<0.01$; *** $p<0.001$, two-tailed *t*-test or one-way ANOVA.

Kragten et al. Figure 3

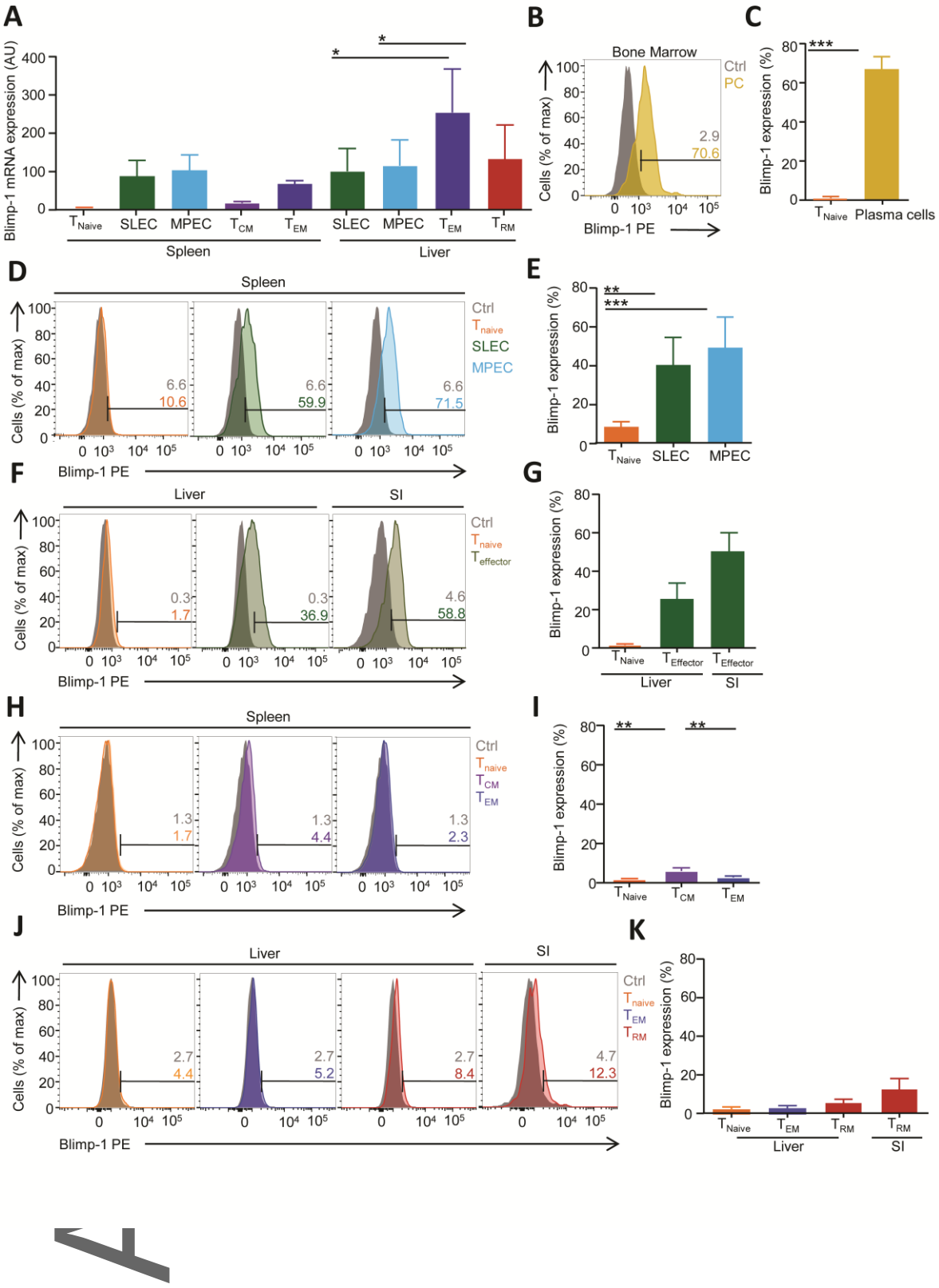

Figure 4: Hobit induces granzyme B expression in memory CD8 T cells after LCMV infection. (A) Histograms depict granzyme B expression in WT (dark green) and mutant (light green) virus-specific CD8 T cells of *Blimp-1* KO (left panel) and *Hobit* KO mice (right panel) at day 8 after infection with LCMV-WE. Numbers indicate percentage of granzyme B expressing CD8 T cells. (B) The percentage of effector CD8 T cells that express granzyme B was quantified in WT (dark green) and *Blimp-1* KO mice (light green, left panel) and in WT (dark green) and *Hobit* KO mice (light green, right panel). (C,D) Similarly, the expression of granzyme B was analyzed in virus-specific memory CD8 T cells (Tem in blue, Trm in red) of WT and *Hobit* KO mice at day 61 after infection with LCMV-WE. (C) Contour plots depict the expression of CD69 and granzyme B in the indicated populations of CD8 T cells. (D) The percentage of granzyme B+ cells was quantified in the indicated CD8 T cell populations. (E,F) The expression of (E) granzyme B mRNA and (F) perforin was determined using qPCR in virus-specific CD62L-CD69- Tem and CD62L-CD69+ Trm of WT and *Hobit* KO mice at day 30+ after LCMV infection. (G,H) The degranulation of LCMV-specific CD8 T cells from liver of WT and *Hobit* KO mice was analyzed at day 61 after infection. (G) Histograms and (H) bar graphs display CD107a labeling after brief stimulation with gp33 peptide in LCMV-specific CD8 T cells that were identified using intracellular labeling of IFN-γ. CD62L-CD69- (Tem) and CD62L-CD69+ fractions (Trm) of virus-specific CD8 T cells of WT and *Hobit* KO mice were separately analyzed. Histograms and contour plots in (A, C and G) display representative results from data in (B, D and H), respectively. Data in (B) displays results from one independent experiment out of two with at least three mice per group. Data in (D) displays one representative experiment out of two with four or five mice per group. Data in (E and F) displays pooled results from two experiments with six to eleven mice per group. Data in (H)

displays results from one representative experiment out of two with five mice per group. Data are shown as mean + SEM; *** p < 0.001, two-tailed *t*-test or one-way ANOVA.

Kragten et al. Figure 4

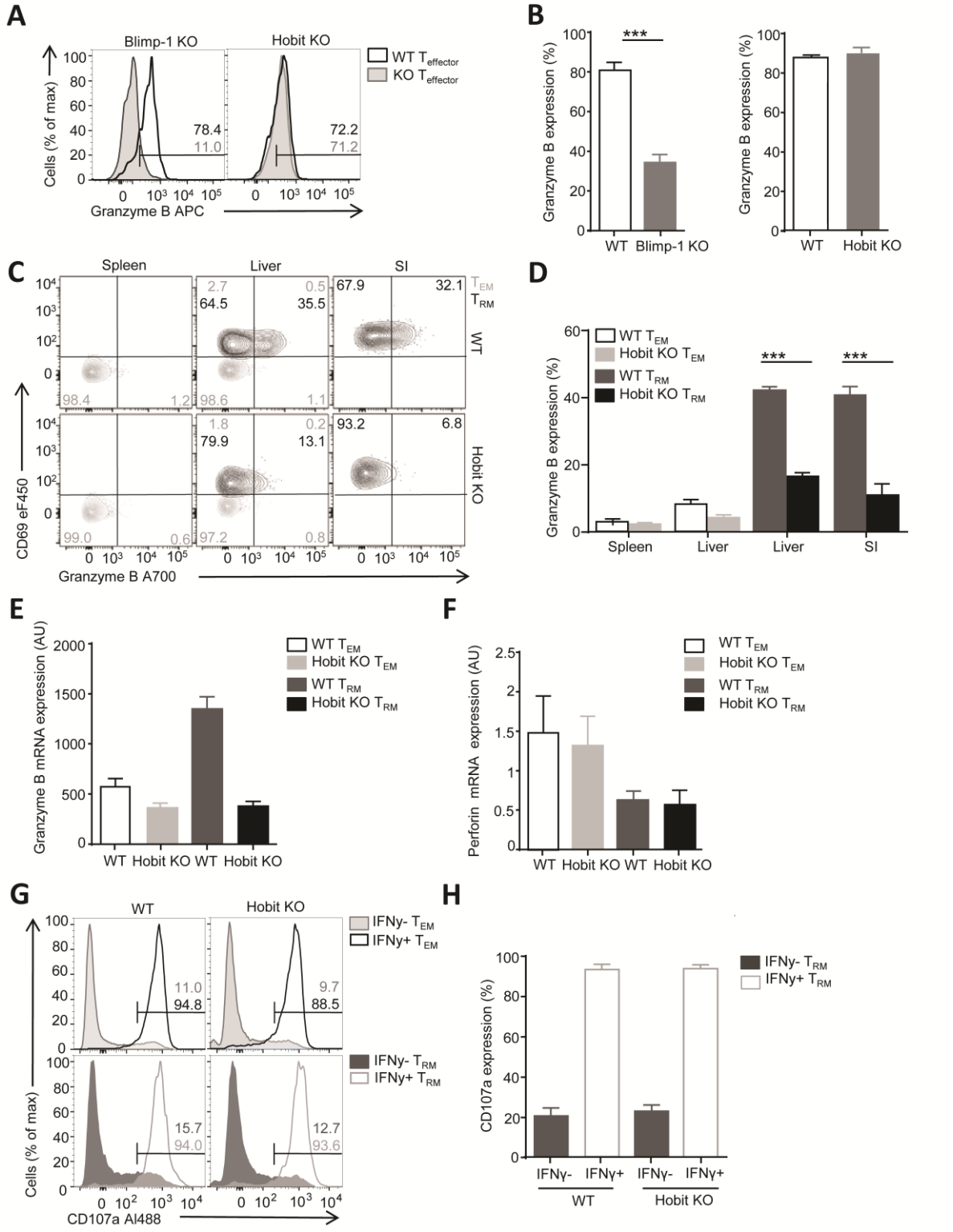

Figure 5: NKT cells constitutively express Blimp-1 mRNA, but require activation to express Blimp-1 protein. (A,B) NKT cells of WT and Blimp-1-GFP reporter mice were stimulated *in vivo* with α-GalCer for 3 days or left unstimulated. (A) The expression of GFP was analyzed in NKT cells of Blimp-1-GFP reporter mice under steady state (filled grey) or after activation with α-GalCer (black line). (B) Isolated NKT cells of WT mice were analyzed for expression of Blimp-1 protein using Western blot under steady state and after activation with α-GalCer. Actin was used as a loading control. (C,D) NKT cells of WT and Blimp-GFP reporter mice were stimulated *in vitro* with anti-CD3/28 and IL-2 for 3 days and with IL-15 for a further 2 (day 5) or 6 days (day 9). (C) The expression of GFP was analyzed at day 5 and 9 in NKT cells of WT (filled grey) and Blimp-1 GFP reporter mice (black line). (D) WT NKT cells were analyzed at day 5 and 9 after culture for expression of Blimp-1 protein using Western blot. Actin was used as a loading control. Histograms in (A, B) display representative data of from at least 2 independent experiments. Western blots in (C, D) display representative data from 3 and 2 independent experiments, respectively.

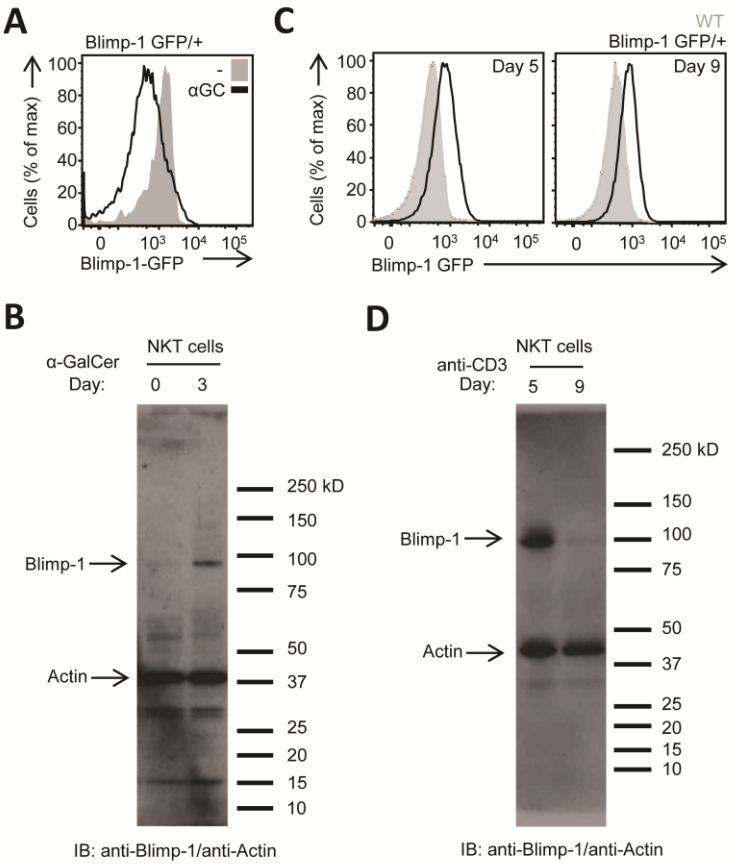

Figure 6: Hobit, but not Blimp-1, maintains granzyme B expression in NKT cells. (A,B) The expression of granzyme B was analyzed in splenic NKT cells under steady state (control) and after *in vivo* stimulation with α-GalCer. (A) Histograms display granzyme B expression in NKT cells of WT (black line) and *Blimp-1* KO mice (filled grey) under the indicated conditions. (B) Bar graphs depict percentage of granzyme B+ NKT cells of the indicated genotypes after α-GalCer stimulation. (C,D) Thymic NKT cells of control WT (Ly5.1+) and of WT, *Hobit* KO and *Blimp-1* KO mice (all Ly5.2+) were isolated using cell sorting and stimulated *in vitro* with anti-CD3/28 and IL-2 and rested in IL-15. (C) Histograms depict granzyme B expression in cultured NKT cells of the indicated genotypes (Ly5.2+, filled grey) compared to that of control WT mice (Ly5.1+, black line). (D) The percentage of granzyme B expression was quantified for cultured NKT cells of the indicated genotypes. (E,F) Cultured NKT cells of control WT (Ly5.1+) mice were intravenously co-injected with NKT cells of WT, *Hobit* KO and *Blimp-1* KO mice (Ly5.2+) into congenically marked WT recipient mice (Ly5.1/2+) and analyzed 18 days after adoptive transfer. (E) Histograms depict granzyme B expression in transferred NKT cells of the indicated genotypes (Ly5.2+, filled grey) compared to that of control WT mice (Ly5.1+, black line). (F) The percentage of granzyme B expression was quantified in donor NKT cells of the indicated genotypes. Histograms in (A, C, E) display representative data from results in (B, D, F). Data in (B, D, F) represent 1 experiment out of at least 2 with at least 3 mice per group. Data are shown as mean + SEM; * $p<0.05$; *** $p<0.001$, two-tailed t-test or one-way ANOVA.

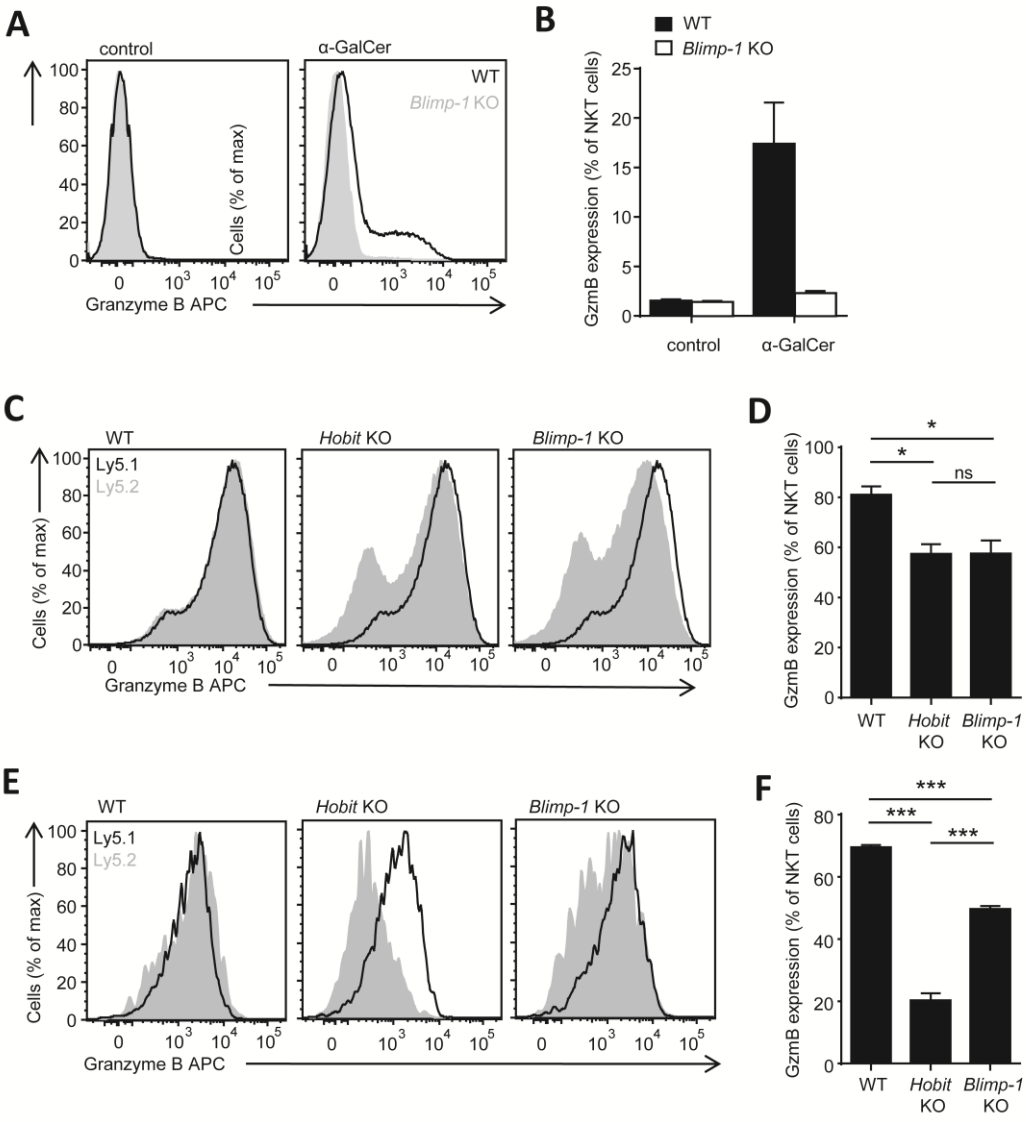

Figure 7: Blimp-1 expression is not maintained at the protein level in human memory CD8 T cells. (A) Schematic representation displays the culture protocol of CD8 T cells. (B,C) CD8 T cells were sorted based on expression of CD27 and CD45RA into naive (CD27+CD45RA+), memory (CD27+CD45RA-) and effector (CD27-CD45RA+) populations. Isolated CD8 T cells were not activated (control) or activated with anti-CD3/CD28 antibodies and IL-2 for 3 days. (B) Blimp-1 mRNA expression was analyzed in naive (left panel), memory (center panel) and effector CD8 T cells (right panel) under the indicated conditions. (C) Blimp-1 protein expression (top lane) was analyzed by Western blot in naive (left panel) and memory CD8 T cells (right panel) under the indicated conditions. β-actin was used as a loading control (bottom lane). (D,E) Naive CD8 T cells were activated with anti-CD3/CD28 antibodies and IL-2 for 3 days and analyzed directly or analyzed after further culture in IL-15 for 7 or 8 days. (D) Blimp-1 mRNA was analyzed using qPCR and (E) Blimp-1 protein was analyzed using Western blot. β-actin was used as a loading control (bottom lane). Data displayed in (B) represents five donors from two independent experiments. Data in (C, D and E) display one representative experiment out of at least two independent experiments. The representative experiment in (D) contained four donors. * $p < 0.05$, two-tailed *t*-test.

Kragten et al. Figure 7

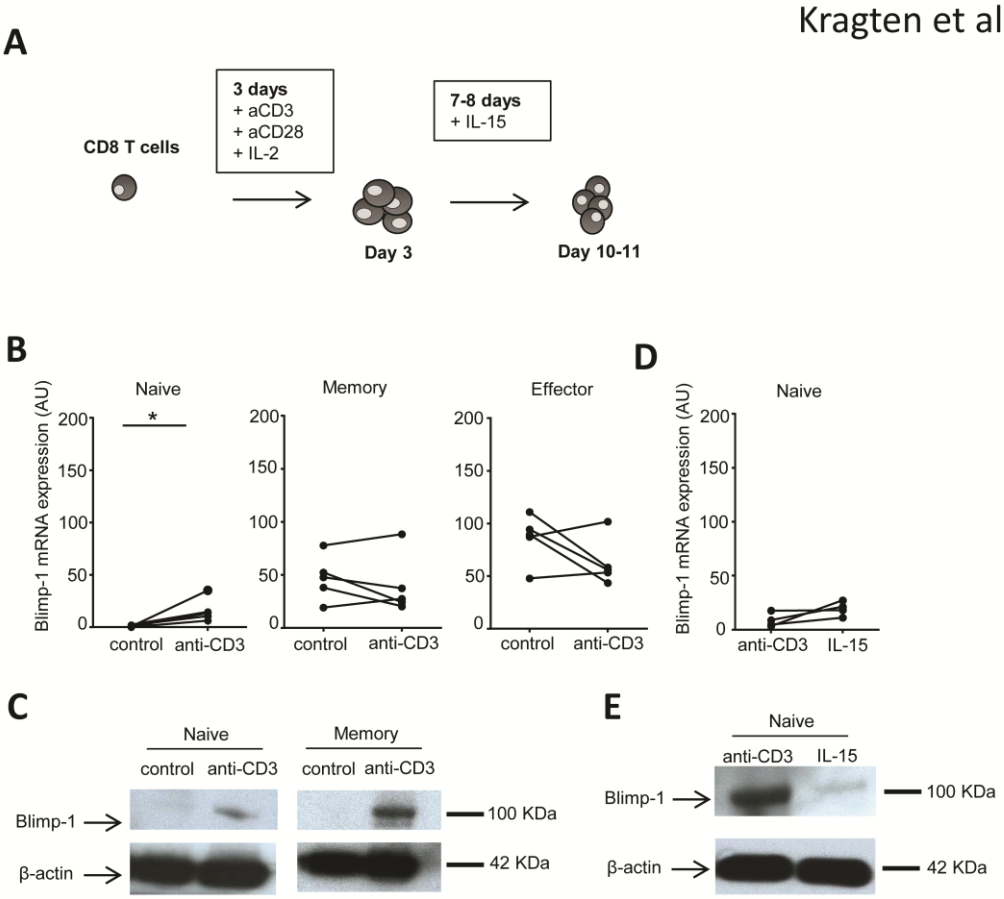

Figure 8: Hobit is co-expressed with perforin and granzyme B or K in human CD8 T cells. (A,B) The co-expression of Hobit and granzyme B was analyzed by flow cytometry in CD8 T cells of human peripheral blood. (A) Dot plot depicts Hobit and granzyme B expression in CD8 T cells of a representative donor. Numbers represent percentage of cells within quadrant. (B) The percentage of CD8 T cells expressing only granzyme B (in yellow), only Hobit (in red), or both Hobit and granzyme B (in black) was quantified. (C) Histograms and (D) bar graphs depict the expression of perforin (left panels) and granzyme K (right panels) of Hobit-granzyme B- (blue), Hobit+granzyme B- (red) and Hobit+granzyme B+ (black) CD8 T cells. Data in (A and C) show a representative example from data in (B and D), respectively. Data in (B) displays the pooled results of nine donors from two experiments and data in (D) displays data of 4 donors from one representative experiment out of two. Data are shown as mean + SEM; *** $p < 0.001$, one-way ANOVA.

Kragten et al: Figure 8

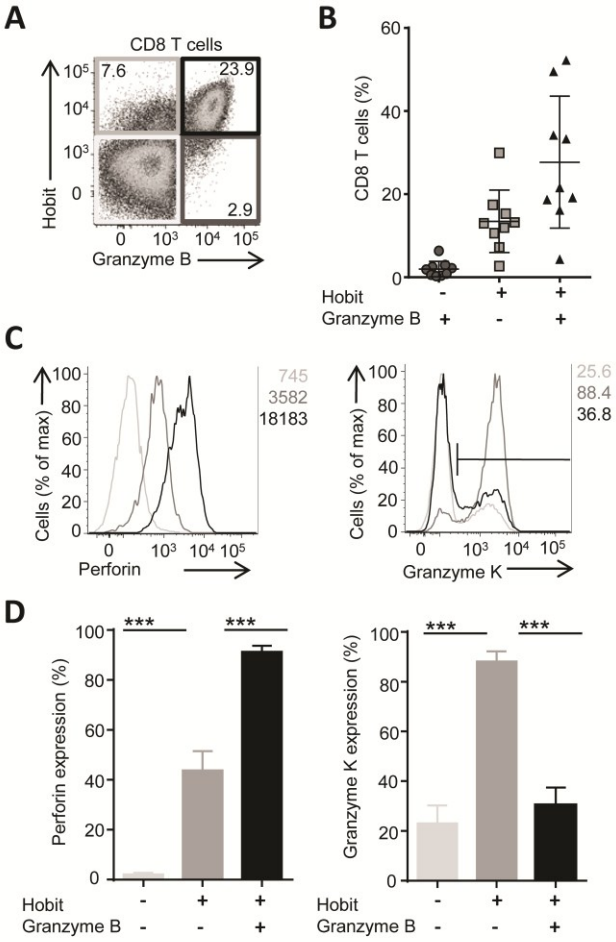

Figure 9. Activation induces downregulation of Hobit expression at the transcriptional level in human CD8 T cells. (A-C) Naive (CD27+CD45RA+) and effector CD8 T cells (CD27-CD45RA+) were isolated using cell sorting and left unstimulated (control) or stimulated with anti-CD3/CD28 antibodies and IL-2. The expression of Hobit was determined using (A) qPCR and (B) flow cytometry in naive (left panels) and effector CD8 T cells (right panels) under the indicated conditions. (C) Histograms display binding of secondary antibodies (control; filled grey) and expression of Hobit (black line) in naive and effector CD8 T cells under the indicated conditions. Numbers in upper right corner display geometric mean fluorescence intensity (geo MFI) of Hobit expression. (D-F) Isolated effector CD8 T cells were left unstimulated (control) or were briefly stimulated with PMA and ionomycin. The expression of Hobit was determined using (D) qPCR and (E) flow cytometry. (F) Histogram displays Hobit expression of effector CD8 T cells under the indicated conditions. Numbers in upper left corner display geo MFI of Hobit expression. (G) The expression of Hobit was determined in the Ki67low and Ki67high fractions of hCMV (TPR) and EBV (EPL) specific CD8 T cells at the indicated time-points after transplantation of a hCMV+ and EBV+ kidney into an hCMV- and EBV- recipient. Dot plots display tetramer binding and Ki67 expression in CD8 T cells at the indicated weeks (Wk) after transplantation (Tx). Numbers on top of gates represent percentage of cells. Histograms depict Hobit expression in Ki67low and Ki67high tetramer+ CD8 T cells. Numbers in upper left corner represent geo MFI of Hobit expression. (H) The expression of Hobit and granzyme B (top row) and Blimp-1 and granzyme B (bottom row) was determined in isolated naive (grey dots) and effector CD8 T cells (black dots) under steady state (control, left panels) and after activation with anti-CD3/CD28 antibodies and IL-2 (right panels). Data in (A) display five donors from two independent experiments. Data in (B) display one representative experiment with three donors out of three independent

experiments. Histograms in (C) show one representative donor from the data displayed in (B). Data in (D and E) display at least six donors from three separate experiments. Histograms in (F) show one representative donor from the data displayed in (E). Data in (G) are representative of two donors and data in (H) are representative of five donors from two independent experiments. * $p<0.05$; ** $p<0.01$, two-tailed *t*-test.

Kragten et al: Figure 9

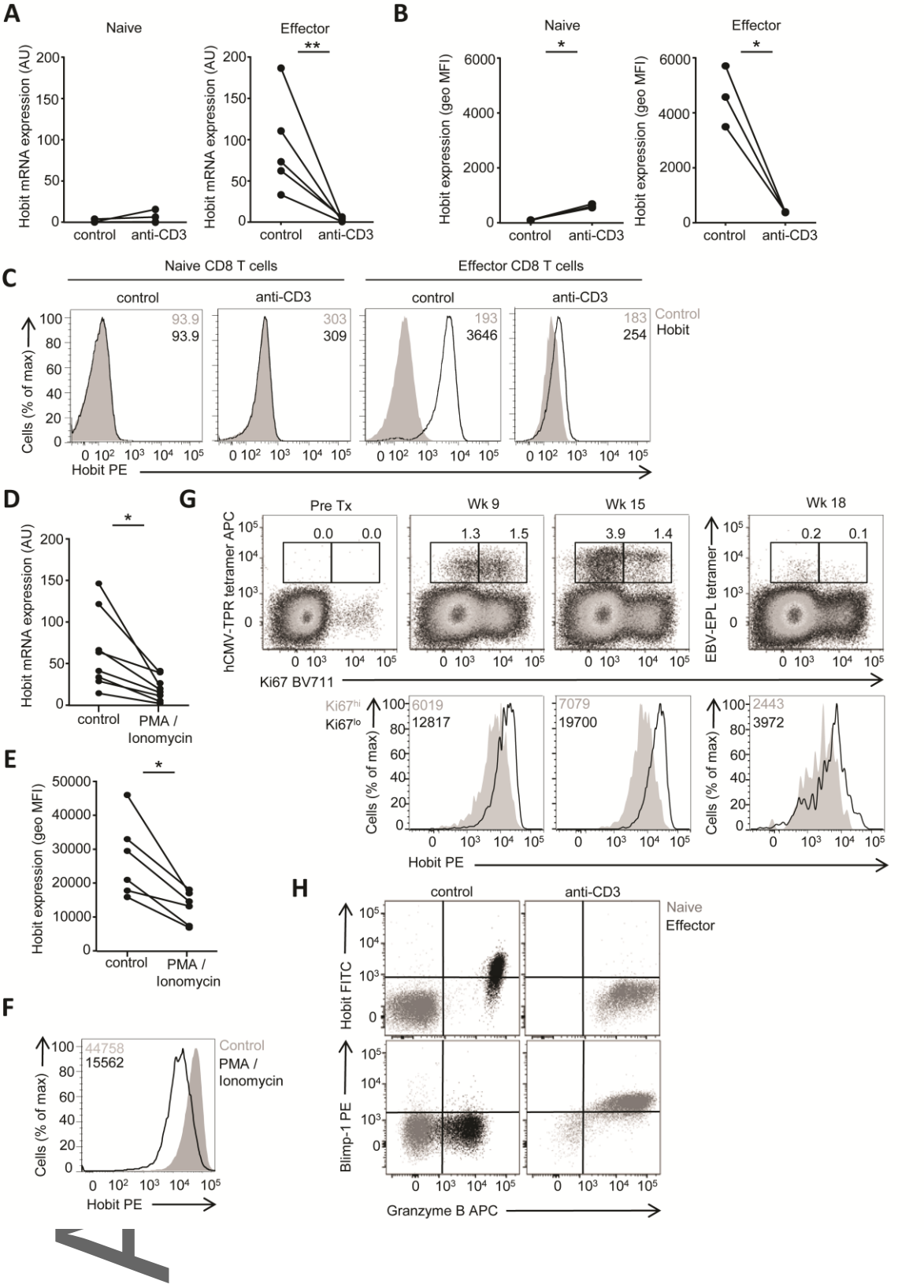

Graphical abstract statements:

Blimp-1 expression is maintained at the mRNA level, but not at the protein level, during quiescence.

The Blimp-1 homologue Hobit is maintained at mRNA and protein level during quiescence.

Tissue-resident memory CD8 T cells maintain granzyme B expression and cytotoxicity.

Hobit regulates expression of granzyme B in tissue-resident memory CD8 T cells during steady state.